Transportation Research Part E 48 (2012) 701–714

Contents lists available at SciVerse ScienceDirect

Transportation Research Part E

journal homepage: www.elsevier.com/locate/tre

# Sailing speed optimization for container ships in a liner shipping network

Shuaian Wang, Qiang Meng *

*Department of Civil and Environmental Engineering, National University of Singapore, Singapore 117576, Singapore*

ARTICLE INFO

*Article history:*
Received 15 July 2011
Received in revised form 2 October 2011
Accepted 14 December 2011

*Keywords:*
Container liner shipping
Sailing speed
Bunker
Outer-approximation

ABSTRACT

This paper first calibrates the bunker consumption – sailing speed relation for container ships using historical operating data from a global liner shipping company. It proceeds to investigate the optimal sailing speed of container ships on each leg of each ship route in a liner shipping network while considering transshipment and container routing. This problem is formulated as a mixed-integer nonlinear programming model. In view of the convexity, non-negativity, and univariate properties of the bunker consumption function, an efficient outer-approximation method is proposed to obtain an $\varepsilon$-optimal solution with a predetermined optimality tolerance level $\varepsilon$. The proposed model and algorithm is applied to a real case study for a global liner shipping company.



## 1. Introduction

Liner shipping companies transport containers with fixed schedules. The arrival date at each port of call is published and usually remains unchanged for a period of 3–6 months. Once the liner shipping services are designed, the inter-arrival time between two adjacent ports of call and thereby the sailing speed of container ships is also determined. The sailing speed of container ships has a significant impact on the total operating cost. On one hand, bunker consumption of a container ship is very sensitive with its sailing speed: daily bunker consumption is approximately proportional to the third power of sailing speed (Ronen, 1982). On the other hand, the bunker cost accounts for a large proportion of the total operating cost, for example, 20–60% according to Ronen (1993). In recent years, bunker price is very high due to the high crude oil price. Consequently, bunker cost is estimated to be 50% (Notteboom, 2006) or even more than 60% (Golias et al., 2009) of the total operating cost of a liner shipping company.

The sailing speed also affects round-trip time of a ship route. For instance, if the round-trip time of a ship route is 56 days when container ships sail at 24 knots, the round-trip time might be increased to more than 56 days, say, 63 days, when container ships sail at a lower speed. Since the liner shipping company generally provides weekly shipping services, the number of container ships deployed on the ship route will increase from 8 to 9. Therefore, slow steaming leads to less bunker consumption, whereas more container ships may be needed to provide weekly service frequency. As a result, liner shipping companies choose a low speed in order to save the bunker cost under two circumstances: (i) when the bunker price is extremely high, or (ii) when a large number of container ships are in lay-up. For example, both the Grand Alliance and CMA CGM each decided to add a ninth ship to one of their respective Asia–Europe routes during the summer of 2006 to cope with the high bunker price. The resulting bunker cost savings generated by each of the other eight vessels more than compensated for the cost of hiring and operating the ninth vessel (Vernimmen et al., 2007). Another example is that in 2009, to deal with the decreased container shipment demand and the large container ship fleet, liner shipping companies took measures including slow or super slow steaming (at half speed of around 13 knots) in an attempt to curb shipping capacity and thus boost the freight rate (UNCTAD, 2010).

* Corresponding author. Tel.: +65 6516 5494; fax: +65 6779 1635.
*E-mail address:* ceemq@nus.edu.sg (Q. Meng).

1366-5545/$ - see front matter 
doi:10.1016/j.tre.2011.12.003

The round-trip time of a ship route is fixed once the number of ships deployed is determined. The round-trip time consists of sailing time at sea and port time. A large proportion of the port time is used for container handling. The total container handling time at all ports of call on a ship route depends on how containers are transported from origin to destination. Because of transshipment, containers can be transported from origin port to destination port on many different paths which are referred to as container routes hereafter. The choice of container routes to transport containers has an important bearing on the total port time of each ship route. Therefore, container routing also has implications on sailing speed and bunker consumption. The purpose of this paper is to investigate the optimal sailing speed of container ships and the optimal number of ships to deploy on each ship route in a liner shipping network while considering container routing.

### 1.1. Literature review

Most studies on optimization of liner shipping services have assumed that ships sail at a given speed (Christiansen et al., 2004; Shintani et al., 2007; Gelareh et al., 2010; Gelareh and Pisinger, 2011; Meng and Wang, 2011a,b; Wang et al., 2011; Wang and Meng, 2011, 2012). Engine theory and empirical data demonstrate that the daily bunker consumption of a ship is approximately proportional to the third power of its sailing speed (Ronen, 1982). Based on the third power relationship, some researchers (Corbett et al., 2010; Meng and Wang, 2010, 2011c; Ronen, 2011) have investigated the optimal sailing speed issue of container ships for a single ship route. Methods used in research related to optimizing sailing speed in a more general environment can be classified into four categories. The first approach bypasses the nonlinearity by assuming that the bunker consumption varies linearly with the sailing speed (Lang and Veenstra, 2010). This approach is a good approximation only when the possible speed range is very narrow. The second approach is heuristic method, like genetic algorithm used in Golias et al. (2010), which cannot guarantee optimality. Discretizing the sailing speed range is the third approach to address the nonlinearity (Gelareh and Meng, 2010; Alvarez et al., 2010). This general method is applicable to almost all the continuous nonlinear functions and can control the approximation error by the number of discretization intervals. Nevertheless, the large problem instances can be hardly solved with acceptable precision because the large number of binary decision variables for indicating each speed interval would lead to a drastic increase in computational burden. Du et al. (2011) proposed a new algorithm by exploiting the property of the power relation between bunker consumption and sailing speed. They transformed the constraints with power functions to the second-order cone programming (SOCP) constraints and take advantage of state-of-art solvers to solve the SOCP problem. This exact algorithm is efficient when the power of speed in the bunker consumption function takes some specific values such as 3.5, 4.0, or 4.5. When the power takes other values, say, 3.31, each power function constraint has to be represented by a substantial number of the SOCP constraints and the problem can no longer be solved efficiently.

### 1.2. Objectives

Although many research works have used the third power relationship, we are aware of no studies that provide empirical data to show how good the third power approximation is. Notteboom and Vernimmen (2009) plotted the bunker consumption – sailing speed curve based on real data, whereas they only mentioned that an increase in sailing speed with just a couple of knots would result in a dramatic increase of bunker consumption. Therefore, the first objective of this study is to close the gap in literature by examining the bunker consumption – sailing speed relation using historical operating data from a global liner shipping company. The second objective of this paper is to investigate the optimal sailing speed problem of container ships on each leg of ship routes in a liner shipping network. Practical issues which are seldom examined by existing studies on the speed optimization, including unique bunker consumption function for each leg, transshipment, container routing, and container handling time, are taken into account in the model. The sailing speed optimization problem for container ships in a liner shipping network with container routing is a practical research issue arising in the liner shipping industry. This problem is formulated as a mixed-integer nonlinear programming model. In view of the convexity, non-negativity, and univariate properties of the bunker consumption – sailing speed function, a novel outer-approximation algorithm is proposed to obtain an $\varepsilon$-optimal solution. Similar to the discretization method (Gelareh and Meng, 2010; Alvarez et al., 2010) or the SOCP approach (Du et al., 2011), the proposed algorithm is exact in that it obtains an $\varepsilon$-optimal solution. At the same time, the outer-approximation algorithm is very efficient compared to the discretization method and not subject to the restriction of the SOCP approach.

The remainder of this paper is organized as follows. Section 2 calibrates the bunker consumption – sailing speed relation using historical operating data from a global liner shipping company. Section 3 examines the sailing speed optimization problem in a liner shipping network by taking into account container routing. A mixed-integer nonlinear programming model is developed. Section 4 analyzes the structure of the problem and proposes an exact and efficient outer-approximation method. Section 5 carries out a real-case study to demonstrate applicability and efficiency of the algorithm. Conclusions are presented in Section 6.

## 2. Calibration of bunker consumption – sailing speed function

According to the literature review, we assume that the daily bunker consumption $Q$ (tons/day) and sailing speed $v$ (knot) has the power relationship:

$$Q = a \times v^b \tag{1}$$

where $a$ and $b$ are coefficients to be calibrated from real data. Function (1) is more general than the third power relation assumed in most existing studies. We can transform Eq. (1) into an equivalent form:

$$\ln Q = \ln a + b \times \ln v \tag{2}$$

Therefore, we can consider $\ln v$ as the independent variable and $\ln Q$ as the response variable, and use the conventional linear regression method to calibrate parameters $\ln a$ and $b$.

### 2.1. Data description

We take advantage of five groups of data provided by a global liner shipping company as shown in Table 1. This dataset is representative because it covers three types of ships – 3000-TEU (acronym for 20-foot equivalent unit), 5000-TEU, and 8000-

**Table 1**
Historical data on sailing speed and bunker consumption.

| Ship type and voyage leg | Average speed (knot) | Bunker (ton/day) | Average speed (knot) | Bunker (ton) |
|---|---|---|---|---|
| 3000-TEU Singapore–Jakarta (SG–JK) | 16.0 | 42 | 17.3 | 53 |
| | 17.0 | 47 | 16.9 | 47 |
| | 16.3 | 43 | 15.7 | 39 |
| | 15.0 | 37 | 17.1 | 50 |
| | 17.6 | 56 | 18.0 | 60 |
| | 16.4 | 44 | 16.2 | 43 |
| | 15.9 | 40 | 17.5 | 55 |
| | 15.5 | 38 | 15.8 | 39 |
| | 16.6 | 45 | 15.4 | 38 |
| | 17.7 | 58 | 16.5 | 45 |
| 3000-TEU Singapore–Kaohsiung (SG–KS) | 20.0 | 82 | 18.7 | 69 |
| | 20.5 | 87 | 20.7 | 93 |
| | 18.5 | 67 | 19.0 | 73 |
| | 19.7 | 77 | 20.6 | 90 |
| | 19.6 | 76 | 19.8 | 78 |
| | 18.8 | 72 | 20.4 | 85 |
| | 20.9 | 98 | 19.4 | 75 |
| | 20.8 | 96 | 21.5 | 108 |
| | 18.2 | 65 | 21.1 | 101 |
| | 21.2 | 103 | 20.3 | 84 |
| 5000-TEU Hong Kong–Singapore (HK–SG) | 17.0 | 51 | 17.0 | 51 |
| | 18.5 | 70 | 16.8 | 48 |
| | 17.9 | 64 | 16.5 | 46 |
| | 17.4 | 56 | 17.0 | 52 |
| | 16.9 | 49 | 18.9 | 74 |
| | 16.4 | 46 | 17.1 | 53 |
| | 17.1 | 52 | 18.5 | 71 |
| | 16.1 | 45 | 17.6 | 59 |
| | 19.8 | 80 | 18.4 | 69 |
| | 19.0 | 75 | 18.2 | 67 |
| 8000-TEU Yantian–Los Angeles (YT–LA) | 19.0 | 109 | 19.6 | 121 |
| | 19.5 | 118 | 18.4 | 98 |
| | 18.8 | 103 | 18.5 | 100 |
| | 21.0 | 147 | 21.4 | 155 |
| | 19.7 | 123 | 22.0 | 178 |
| | 20.4 | 135 | 20.2 | 132 |
| | 18.9 | 106 | 19.7 | 124 |
| | 17.9 | 89 | 19.4 | 117 |
| | 19.3 | 115 | 18.9 | 105 |
| | 17.0 | 81 | 23.0 | 200 |
| 8000-TEU Tokyo–Xiamen (TK–XM) | 17.5 | 86 | 18.4 | 97 |
| | 17.8 | 87 | 17.4 | 85 |
| | 16.8 | 76 | 18.0 | 92 |
| | 20.1 | 128 | 17.0 | 82 |
| | 16.1 | 70 | 18.6 | 102 |
| | 15.8 | 68 | 17.2 | 83 |
| | 21.0 | 146 | 16.9 | 79 |
| | 20.5 | 135 | 18.0 | 93 |
| | 16.5 | 75 | 17.8 | 88 |
| | 17.2 | 84 | 17.0 | 81 |

TEU ships – on five voyage legs. There are 20 historical data for each voyage leg on the average sailing speed and daily bunker consumption. We hence calibrate the parameter $a$ and $b$ for each group of data using the linear regression method.

### 2.2. Calibration results with statistical analysis

Fig. 1 shows the calibrated bunker consumption – sailing speed function, the historical operating data (the diamonds) and the calibrated function (the curve). Table 2 reports the calibration and relevant statistical test results. First, we observe that the coefficient of determination $R^2$ is at least 0.96 and the adjusted $R^2$ is at least 0.95. Also, at the 5% significance level, the hypothesis that the residual errors are normally distributed is not rejected for any of the five data sets by using the Anderson–Darling Test. Therefore, using the power function (1) to approximate the bunker consumption function is appropriate.

Second, at the 5% significance level, the hypothesis that $b = 1$ is rejected for all of the five data sets as shown in Table 2. We can hence conclude that the daily bunker consumption is a not a linear function of the sailing speed. Table 2 also shows that at the 5% significance level, the hypothesis that $b = 3$ is rejected for two of the five data sets. Among the five data sets, the

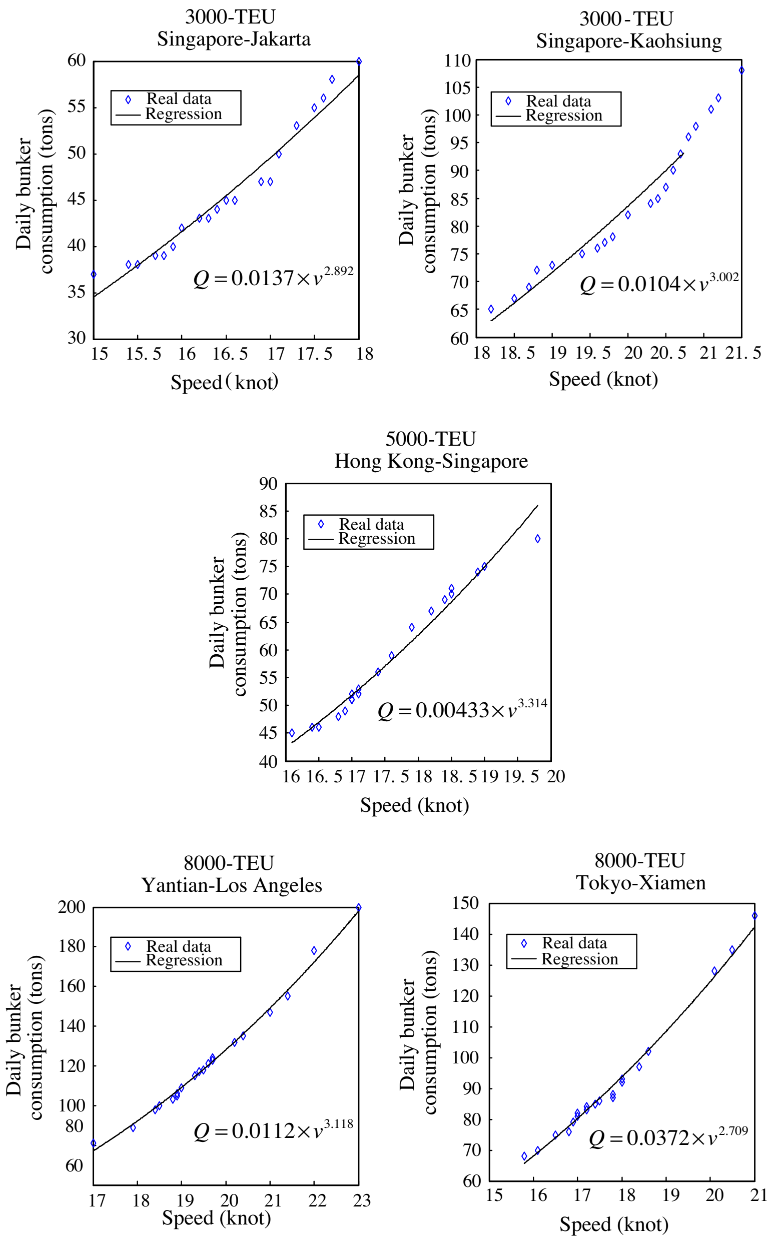


**Fig. 1.** Bunker consumption – sailing speed relation.

**Table 2**
Statistical analysis of the linear regression model.

| | | 3000-TEU SG-JK | 3000-TEU SG-KS | 5000-TEU HK-SG | 8000-TEU YT-LA | 8000-TEU TK-XM |
|---|---|---|---|---|---|---|
| | $a$[a] | 0.014 | 0.010 | 0.004 | 0.011 | 0.037 |
| | $b$ | 2.892 | 3.002 | 3.314 | 3.118 | 2.709 |
| | $R^2$ | 0.964 | 0.960 | 0.977 | 0.993 | 0.990 |
| | Adjusted $R^2$ | 0.962 | 0.958 | 0.976 | 0.993 | 0.990 |
| $p$-values | $H_0$: $b = 1$[b] | 0.000 | 0.000 | 0.000 | 0.000 | 0.000 |
| | $H_0$: $b = 3$[c] | 0.425 | 0.990 | 0.018 | 0.066 | 0.000 |
| | Normality of residual error[d] | 0.790 | 0.095 | 0.112 | 0.150 | 0.638 |

[a] Computed from ln $a$.
[b] $t$-Test.
[c] $t$-Test.
[d] Anderson–Darling test.

largest coefficient $b$ is 3.3 and the smallest is 2.7. As a consequence, we reach the conclusion that the third power relationship is indeed a good approximation. Nevertheless, we argue that the third power relation can be used if not enough historical data are available. Once enough historical data are ready for obtaining $b$ through regression, we should use a more accurate bunker consumption function.

Third, the regression analysis also shows that bunker consumption is dependent on voyage legs. For example, the bunker consumption – sailing speed functions for 3000-TEU ships on the leg Singapore–Jakarta and the leg Singapore–Kaohsiung are different. This can be explained by the fact that different legs have different weather conditions and sea conditions such as currents. As a consequence, the optimal sailing speeds on different legs may be different.

## 3. Sailing speed optimization problem

### 3.1. Weekly-service based ship route, sailing speed, and bunker consumption

Consider a liner container shipping company which operates a group of ship routes denoted by the set $\mathcal{R}$ to regularly serve a group of ports denoted by the set $\mathcal{P}$. The itinerary (or port rotation) of a ship route forms a loop in practice, and a port may be visited for more than one time by a container ship serving the ship route during a round trip. Let $N_r$ denote the number of ports of call on a ship route $r \in \mathcal{R}$ and $p_{ri} \in \mathcal{P}$ be the port corresponding to the $i$th port of call. The port rotation of the ship route $r$ can thus be expressed as follows:

$$p_{r1} \to p_{r2} \to \cdots \to p_{rN_r} \to p_{r1} \tag{3}$$

Let $\mathcal{I}_r = \{1, 2, \ldots, N_r\}$ be the set of all the port of call indices for the ship route $r$. Defining $p_{r,N_r+1} = p_{r1}$, the voyage between two consecutive ports of call $p_{ri}$ and $p_{r,i+1}$ is called *leg i* of the ship route $r$, $i \in \mathcal{I}_r$. Fig. 2 illustrates a liner shipping network with three ship routes elaborated as follows:

$$r = 1,\ N_r = 3 : p_{r1}(\mathrm{HK}) \to p_{r2}(\mathrm{SD}) \to p_{rN_r}(\mathrm{SG}) \to p_{r1}(\mathrm{HK}) \tag{4}$$

$$r = 2,\ N_r = 5 : p_{r1}(\mathrm{HK}) \to p_{r2}(\mathrm{NB}) \to p_{r3}(\mathrm{SG}) \to p_{r4}(\mathrm{CB}) \to p_{rN_r}(\mathrm{SG}) \to p_{r1}(\mathrm{HK}) \tag{5}$$

$$r = 3,\ N_r = 3 : p_{r1}(\mathrm{CB}) \to p_{r2}(\mathrm{NS}) \to p_{rN_r}(\mathrm{CC}) \to p_{r1}(\mathrm{CB}) \tag{6}$$

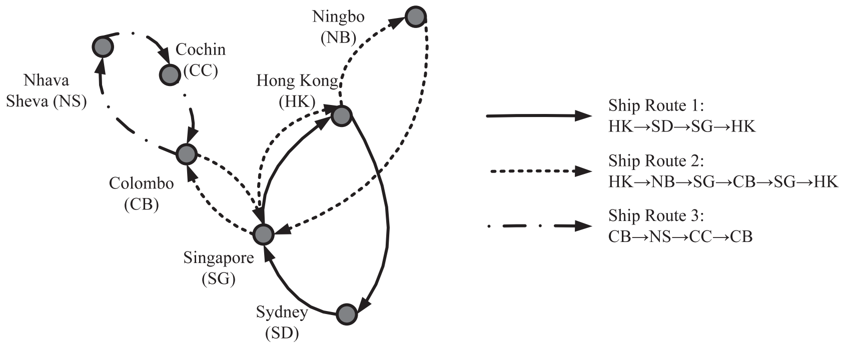


**Fig. 2.** A liner shipping network with three ship routes.

The ship route 1 has three ports of call, i.e., the first port of call (Hong Kong), the second port of call (Sydney), and the third port of call (Singapore). Using the aforementioned notation, $p_{1,1}$ represents the first port of call (Hong Kong) of ship route 1, $p_{1,2}$ represents the second port of call (Sydney), and $p_{1,3}$ represents the third port of call (Singapore). Since a ship route forms a loop, a ship deployed on the ship route 1 returns to the first port of call (Hong Kong) after visiting the third port of call (Singapore). Hence, $N_1 = 3$ and $\mathcal{I}_1 = \{1,2,3\}$ (the subscript 1 denotes ship route 1). Ship route 1 has three legs, i.e., the first leg from $p_{1,1}$ (Hong Kong) to $p_{1,2}$ (Sydney), the second leg from $p_{1,2}$ (Sydney) to $p_{1,3}$ (Singapore), and the third leg from $p_{1,3}$ (Singapore) back to $p_{1,1}$ (Hong Kong). On ship route 2, Singapore is visited twice during a round trip. In other words, both the third port of call $p_{2,3}$ and the fifth port of call $p_{2,5}$ refer to Singapore. However, the notation $p_{ri}$ can easily differentiate these two calls: $p_{2,3}$ denotes the call at Singapore after Ningbo, and $p_{2,5}$ denotes the call at Singapore after Colombo.

It is assumed that each ship route $r \in \mathcal{R}$ is deployed with a given type of ship. The capacity of a ship deployed on the ship route $r$ is denoted by $Cap_r$ (TEUs) and let $c_r^{ves}$ (USD/week) be the fixed operating cost of a ship on the ship route $r$. The liner shipping company maintains weekly service frequency on the ship routes. That is, if the round-trip time of a ship route is 42 days, then six ships are deployed to ensure that each port of call is visited one time every week. The round-trip time consists of sea time and port time. The sailing speed on leg $i$ of the ship route $r$, $r \in \mathcal{R}$, $i \in \mathcal{I}_r$, is denoted by $v_{ri}$ (knot). The sailing speed $v_{ri}$ should be within the economic sailing interval $[V_{ri}^{\min}, V_{ri}^{\max}]$. Let $L_{ri}$ be the oceanic distance ($n$ mile) of leg $i$ of the ship route $r$, and the sailing time on leg $i$ is $L_{ri}/v_{ri}$ (h). The port time consists of standby time for pilotage in and out and container handling time. The total standby time for pilotage in and out of ports in a round-trip is denoted by $t_r^{fix}$ (h). Since the weekly service frequency has to be maintained, assuming that a total of $m_r$ ships are deployed on the ship route $r$, we have

$$\sum_{i \in I_r} \frac{L_{ri}}{v_{ri}} + t_r^{fix} + \text{total container handling time at all portcalls} \leqslant 168 m_r, \quad \forall\, r \in \mathcal{R} \tag{7}$$

As the bunker consumption function is dependent on voyage legs, we denote by $g_{ri}(v_{ri})$ (tons/$n$ mile) the bunker consumption per nautical mile at the speed $v_{ri}$ on leg $i$ of ship route $r$. We further use $\alpha^{bun}$ (USD/ton) to represent the bunker fuel price, the total operating cost of the ship route $r$ can thus be calculated by

$$\sum_{i \in I_r} \alpha^{bun} L_{ri} g_{ri}(v_{ri}) + c_r^{ves} m_r \tag{8}$$

### 3.2. Container routing with container transshipment operations

Let $n_{od}$ (TEUs) be the weekly container shipment demand from port $o \in \mathcal{P}$ to port $d \in \mathcal{P}$. Let $\mathcal{W} := \{(o,d) | o \in \mathcal{P}, d \in \mathcal{P}, n_{od} > 0\}$ be the set of origin–destination (O–D) port pairs with container shipment demand. The liner container shipping company predetermines a set of container routes to deliver containers between an O–D port pair $(o,d) \in \mathcal{W}$, denoted by $\mathcal{H}^{od}$, in accordance with the given set of ship routes $\mathcal{R}$. Define $H = \cup_{(o,d)\in\mathcal{W}} \mathcal{H}^{od}$ to be the set of all container routes for all the O–D port pairs. A container route $h \in \mathcal{H}^{od}$ is either a part of one particular ship route or a combination of several ship routes to deliver containers from the original port $o \in \mathcal{P}$ to the destination port $d \in \mathcal{P}$. Container transshipment operations should be involved in a container route with several ship routes. For example, we can design three container routes with respect to the ship routes shown in Fig. 2:

$$h_1 = p_{1,3}(\text{SG}) \xrightarrow{\text{Ship Route1}} p_{1,1}(\text{HK}) \tag{9}$$

$$h_2 = p_{2,5}(\text{SG}) \xrightarrow{\text{Ship Route2}} p_{2,1}(\text{HK}) \tag{10}$$

$$h_3 = p_{2,2}(\text{NB}) \xrightarrow{\text{Ship Route2}} p_{2,4}(\text{CB}) \mapsto p_{3,1}(\text{CB}) \xrightarrow{\text{Ship Route3}} p_{3,2}(\text{NS}) \tag{11}$$

Container route $h_1$ is used to directly deliver containers from Singapore to Hong Kong which are loaded at the 3rd port of call of the ship route 1 (Singapore) and discharged at the 1st port of call of the ship route 1 (Hong Kong). Containers along the container route $h_2$ are delivered by ship route 2. Container route $h_3$ involves container transshipment operations: Containers are first loaded at the 2nd port of call of the ship route 2 (Ningbo) and delivered to the 4th port of call of the ship route 2 (Colombo). At Colombo, these containers are discharged and reloaded (transshipped) to a ship deployed on the ship route 3, and transported to the destination Nhava Sheva.

Each container route contains full information on how containers are transported from the origin port to the destination port. The container routing problem needs to determine how many containers to be transported on each container route $h$, denoted by $y_h$ (TEUs). All container shipment demand has to be fulfilled, namely

$$\sum_{h \in H^{od}} y_h = n_{od}, \quad \forall (o,d) \in \mathcal{W} \tag{12}$$

Let $t_{rh}$ (h/TEU) be the additional round-trip time posed for the ship route $r$ by transporting one TEU according to container route $h$. For instance, each TEU routed on the container route $h_3$ shown by Eq. (11) will be loaded at Ningbo and discharged at Colombo on the ship route 2, thereby increasing the round-trip time of the ship route 2 by the sum of handling time for one

TEU at the two ports: Ningbo and Colombo. Also, each TEU routed on the container route $h_3$ will increase the round-trip time of the ship route 3 by the sum of handling time for one TEU at Colombo and Nhava Sheva. Therefore, the total container handling time (h) at all ports of call on the ship route $r$ can be calculated by

$$\sum_{h\in\mathcal{H}} t_{rh} y_h, \quad \forall\, r \in \mathcal{R} \tag{13}$$

Let $c_h$ (USD/TEU) be the handling cost associated with transporting one TEU on a container route $h$. For instance, $c_{h_3}$ for the container route $h_3$ in Eq. (11) is the sum of loading cost at Ningbo, transshipment cost at Colombo, and discharge cost at Nhava Sheva. Both $t_{rh}$ and $c_h$ are known parameters. The total container handling cost can be calculated by

$$\sum_{h\in H} c_h y_h \tag{14}$$

We further let binary coefficient $\rho_{hri}$ be 1 if containers on the container route $h$ are transported on leg $i$ of ship route $r$, and 0 otherwise. For example, the container route $h_3$ consists of the 2nd and the 3rd legs of the ship route 2 and the 1st leg of the ship route 3. We hence have $\rho_{h_3 22} = 1, \rho_{h_3 23} = 1$, and $\rho_{h_3 31} = 1$. To ensure that ship capacity constraint is respected on all the legs of the ship route $r$, we should have

$$\sum_{h\in H} \rho_{hri} y_h \leqslant \mathrm{Cap}_r, \quad \forall\, r \in \mathcal{R}, \quad \forall\, i \in \mathcal{I}_r \tag{15}$$

### 3.3. Mixed-integer nonlinear programming model

The sailing speed optimization problem can be stated as follows: Given a set of ship routes with fixed port rotations and fixed type of ship to deploy, known container shipment demand between each O–D port pair, and a set of container routes, determine the sailing speed $v_{ri}$ on leg $i$ of a ship route $r$, the number of ships $m_r$ to deploy on the ship route $r$, and the number of containers $y_h$ routed on each container route $h$, in order to fulfill the container shipment demand while minimizing the total operating cost. The port charges and canal dues are fixed; hence we only consider the fixed ship operating cost, bunker cost and container handling cost.

The sailing speed optimization problem can be formulated as a mixed-integer nonlinear programming model [P1]:

$$\text{[P1]} \quad \min_{m_r, v_{ri}, y_h} \sum_{r\in\mathcal{R}} \sum_{i\in I_r} \alpha^{bun} L_{ri} g_{ri}(v_{ri}) + \sum_{r\in\mathcal{R}} c_r^{ves} m_r + \sum_{h\in\mathcal{H}} c_h y_h \tag{16}$$

subject to

$$\sum_{i\in\mathcal{I}_r} \frac{L_{ri}}{v_{ri}} + \sum_{h\in\mathcal{H}} t_{rh} y_h + t_r^{fix} \leqslant 168 m_r, \quad \forall\, r \in \mathcal{R} \tag{17}$$

$$\sum_{h\in\mathcal{H}} \rho_{hri} y_h \leqslant \mathrm{Cap}_r, \quad \forall\, r \in \mathcal{R}, \quad \forall\, i \in \mathcal{I}_r \tag{18}$$

$$\sum_{h\in\mathcal{H}^{od}} y_h = n_{od}, \quad \forall\, (o,d) \in \mathcal{W} \tag{19}$$

$$V_{ri}^{\min} \leqslant v_{ri} \leqslant V_{ri}^{\max}, \quad \forall\, r \in \mathcal{R}, \quad \forall\, i \in \mathcal{I}_r \tag{20}$$

$$m_r \in \mathbb{Z}^+, \quad \forall\, r \in \mathcal{R} \tag{21}$$

$$y_h \geqslant 0, \quad \forall\, h \in \mathcal{H} \tag{22}$$

The objective function (16) minimizes the total operating cost. The first term is the bunker consumption cost, the second term is the vessel operating cost, and the third term is the container handling charges. Constraints (17) enforce the weekly service requirement. Constraints (18) impose the ship capacity constraint. Eq. (19) require that all the container shipment demands are satisfied. Constraints (20) define the lower and upper bounds of sailing speed. Constraints (21) and (22) define $m_r$ as a positive integer variable, and $y_h$ as a nonnegative continuous variable, respectively.

## 4. Solution method

[P1] is a mixed-integer nonlinear programming model with nonlinear terms shown in Eqs. (16) and (17). In order to take advantage of state-of-art mixed-integer linear programming solvers, we intend to linearize the [P1] model. The nonlinearity of Eq. (17) can be overcome by using the reciprocal of sailing speed as a decision variable. We will prove that the nonlinear objective function (16) is convex and therefore an efficient outer-approximation method can be employed by using sum of many piecewise-linear functions to approximate the convex function shown in Eq. (16). The approximation error can be controlled within a predetermined tolerance level with a suitable outer-approximation scheme. Due to the convexity of the objective function, the piecewise-linear approximating functions are also convex. Therefore the model with the sum of the piecewise-linear approximating functions as the objective function can be transformed to a mixed-integer linear programming model. Unlike the discretization approach (Gelareh and Meng, 2010; Alvarez et al., 2010), no additional integer variables are needed. Hence, the mixed-integer linear programming model can be efficiently solved by state-of-art mixed-integer linear programming solvers such as CPLEX.

### 4.1. Alternative decision variables and convexity of objective function

We define new decision variables

$$u_{ri} = 1/v_{ri}, \quad \forall\, r \in \mathcal{R}, \quad \forall\, i \in \mathcal{I}_r \tag{23}$$

All the constraints expressed by Eq. (17) become linear constraints with respect to the alternative decision variable $u_{ri}$:

$$\sum_{i \in \mathcal{I}_r} L_{ri} u_{ri} + \sum_{h \in \mathcal{H}} t_{rh} y_h + t_r^{fix} \leqslant 168 m_r, \quad \forall\, r \in \mathcal{R} \tag{24}$$

The constraints (20) can be rewritten as

$$1/V_{ri}^{\max} = U_{ri}^{\min} \leqslant u_{ri} \leqslant U_{ri}^{\max} = 1/V_{ri}^{\min}, \quad \forall\, r \in \mathcal{R}, \quad \forall\, i \in \mathcal{I}_r \tag{25}$$

The bunker consumption function $g_{ri}(v_{ri})$ can be alternatively expressed as a function of the reciprocal of the sailing speed. We define:

$$Q_{ri}(u_{ri}) = g_{ri}(1/u_{ri}), \quad \forall\, r \in \mathcal{R}, \quad \forall\, i \in \mathcal{I}_r \tag{26}$$

Hence, the model [P1] is equivalent to the following model by rewriting objective function shown in Eq. (16) as a function of the alternative decision variables.

$$[\text{P2}] \quad \min_{m_r, u_{ri}, y_h} \sum_{r \in \mathcal{R}} \sum_{i \in \mathcal{I}_r} \alpha^{\text{bun}} L_{ri} Q_{ri}(u_{ri}) + \sum_{r \in R} c_r^{\text{ves}} m_r + \sum_{h \in \mathcal{H}} c_h y_h \tag{27}$$

subject to constraints (18), (19), (21), (22), (24), and (25).

Note that [P2] is a mixed-integer nonlinear programming model with linear constraints and nonlinear objective function (27).

We exploit the special structure of [P2] and prove that the objective function (27) is convex. To this end, we can prove the convexity of the function $Q_{ri}(u_{ri})$ as a consequence of the convexity, non-negativity, and univariate property of $g_{ri}(v_{ri})$. Suppose that daily bunker consumption (tons) on leg $i$ of ship route $r$ is $a_{ri} \times (v_{ri})^{b_{ri}}$. Noting that $Q_{ri}(u_{ri})$ represents the bunker consumption (tons) per nautical mile, we have

$$Q_{ri}(u_{ri}) = g_{ri}(1/u_{ri}) = \frac{a_{ri} \times (1/u_{ri})^{b_{ri}}}{24 \times (1/u_{ri})} = a_{ri}(u_{ri})^{1-b_{ri}}/24, \quad \forall\, r \in \mathcal{R}, \quad \forall\, i \in \mathcal{I}_r \tag{28}$$

According to the regression analysis, the coefficient $b_{ri}$ is between 2.7 and 3.3 and $a_{ri} > 0$. Therefore $Q_{ri}(u_{ri})$ is convex in $u_{ri}$ on the interval $[U_{ri}^{\min}, U_{ri}^{\max}]$. Even if considering that $b_{ri}$ may be out of the range [2.7, 3.3], $Q_{ri}(u_{ri})$ is convex in $u_{ri}$ as long as $b_{ri} > 1$. Therefore it is reasonable to conclude that the objective function (27) is convex.

### 4.2. Outer-approximation method

In view of the convexity of the function $Q_{ri}(u_{ri})$, we use a piecewise-linear function to approximate it. To control the approximation error, we can define an absolute objective value tolerance $\varepsilon$ (USD/week), namely, the solution obtained by approximation should not be worse than the optimal one by more than $\varepsilon$ in the objective value. In our algorithm, we allocate the total tolerance $\varepsilon$ among the voyage legs in proportion to the voyage distance. Define $\bar{\varepsilon}$ (tons/$n$ mile) as:

$$\bar{\varepsilon} = \frac{\varepsilon}{\alpha^{\text{bun}}} \times \frac{1}{\sum_{r \in R} \sum_{i \in I_r} L_{ri}} \tag{29}$$

If the approximation error for $Q_{ri}(u_{ri})$ is not greater than $\bar{\varepsilon}$, then the overall objective value error is not greater than $\varepsilon$.

Now, we develop an algorithm that generates a piecewise-linear function with as few pieces as possible for approximating $Q_{ri}(u_{ri})$ while controlling the approximation error within $\bar{\varepsilon}$ for any $u_{ri} \in [U_{ri}^{\min}, U_{ri}^{\max}]$. Let $Q'_{ri}(u_{ri})$ denote the derivative of $Q_{ri}(u_{ri})$ at $u_{ri}$, namely

$$Q'_{ri}(u_{ri}) = a_{ri}(1 - b_{ri})(u_{ri})^{-b_{ri}}/24 \tag{30}$$

We describe the algorithm below by using Fig. 3 to schematically illustrate it.

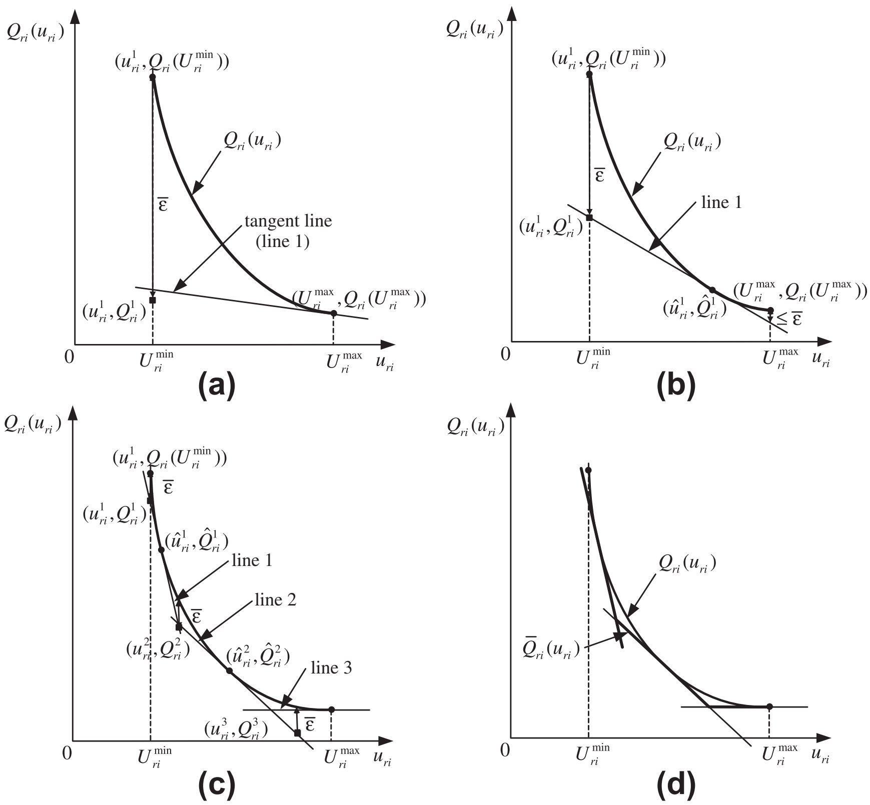

**Fig. 3.** Generation of a piecewise-linear approximation function.

**Algorithm 1.** Generation of a piecewise-linear approximation function

*Step 0:* Let $\Psi$ be a set of lines, $\Psi = \varnothing$. Set $k = 0$, $u_{ri}^1 = U_{ri}^{\min}$, $Q_{ri}^1 = Q_{ri}(u_{ri}^1) - \bar{\varepsilon}$.
*Step 1:* Set $k = k + 1$. If the following inequality holds:

$$\frac{Q_{ri}(U_{ri}^{\max}) - Q_{ri}^k}{U_{ri}^{\max} - u_{ri}^k} \geqslant Q'_{ri}(U_{ri}^{\max}) \tag{31}$$

namely, point $(u_{ri}^k, Q_{ri}(u_{ri}^k))$ is on or below the tangent line of $Q_{ri}(u_{ri})$ at $U_{ri}^{\max}$, see Fig. 3a, add to $\Psi$ line $k$ as follows

$$Q_{ri} - Q_{ri}(U_{ri}^{\max}) = Q'_{ri}(U_{ri}^{\max})(u_{ri} - U_{ri}^{\max}) \tag{32}$$

and go to Step 3. Else, add to $\Psi$ line $k$ that passes the point $(u_{ri}^k, Q_{ri}^k)$ and supports the epigraph of $Q_{ri}(u_{ri})$. Line $k$ can be obtained in the following manner. Suppose that line $k$ supports the epigraph of $Q_{ri}(u_{ri})$ at the point $(\hat{u}_{ri}^k, \widehat{Q}_{ri}^k)$. According to Eq. (28) we have

$$\widehat{Q}_{ri}^k = a_{ri}(\hat{u}_{ri}^k)^{1-b_{ri}}/24 \tag{33}$$

By definition,

$$\frac{\widehat{Q}_{ri}^k - Q_{ri}^k}{\hat{u}_{ri}^k - u_{ri}^k} = Q'_{ri}(\hat{u}_{ri}^k) = a_{ri}(1 - b_{ri})(\hat{u}_{ri}^k)^{-b_{ri}}/24 \tag{34}$$

Combining Eqs. (33) and (34), we can numerically estimate $\hat{u}_{ri}^k$ by the bisection search method. Hence, line $k$ is defined to be

$$Q_{ri} - Q_{ri}^k = \frac{\widehat{Q}_{ri}^k - Q_{ri}^k}{\hat{u}_{ri}^k - u_{ri}^k}(u_{ri} - u_{ri}^k) \tag{35}$$

Go to Step 2.
*Step 2:* For line $k$, when $u_{ri}$ takes the value $U_{ri}^{\max}$, $Q_{ri}$ will take the following value:

$$Q_{ri}^k + \frac{\widehat{Q}_{ri}^k - Q_{ri}^k}{\hat{u}_{ri}^k - u_{ri}^k}(U_{ri}^{\max} - u_{ri}^k) \tag{36}$$

If Eq. (36) is not less than $Q_{ri}(U_{ri}^{\max}) - \bar{\varepsilon}$, namely, the gap between line $k$ and function $Q_{ri}(u_{ri})$ is not greater than $\bar{\varepsilon}$ even when $u_{ri}$ takes the value $U_{ri}^{\max}$, then we can conclude that the gap between line $k$ and function $Q_{ri}(u_{ri})$ is not greater than $\bar{\varepsilon}$ when $u_{ri}$ takes any value between $u_{ri}^k$ and $U_{ri}^{\max}$, see Fig. 3b, go to Step 3. Else, there exists exactly one point $(u_{ri}^{k+1}, Q_{ri}^{k+1})$ on line $k$ such that $u_{ri}^k < u_{ri}^{k+1} < U_{ri}^{\max}$ and $Q_{ri}^{k+1} = Q_{ri}(u_{ri}^{k+1}) - \bar{\varepsilon}$, see Fig. 3c. Similar to $\hat{u}_{ri}^k$, $u_{ri}^{k+1}$ can also be numerically estimated by bisection search method. Go to Step 1.

*Step 3:* Let $K_{ri}$ be the current value of $k$, namely, the number of lines in $\Psi$, and use the generic form

$$Q_{ri} = \text{slope}_{rik} \times u_{ri} + \text{Q-intercept}_{rik} \tag{37}$$

to represent a line $k$ in $\Psi$ that is defined by Eqs. (32) and (35), $k = 1, 2, \ldots, K_{ri}$. The piecewise-linear approximation function represented by $\overline{Q}_{ri}(u_{ri})$ can be written as

$$\overline{Q}_{ri}(u_{ri}) = \max\{\text{slope}_{rik} \times u_{ri} + \text{Q-intercept}_{rik},\ k = 1, 2 \ldots K_{ri}\} \tag{38}$$

$\overline{Q}_{ri}(u_{ri})$ is schematically shown by the thickest solid line in Fig. 3d.

We can replace $Q_{ri}(u_{ri})$ in the objective function (27) of [P2] by $\overline{Q}_{ri}(u_{ri})$ and obtain an approximation model represented by [P3]:

$$[\text{P3}] \quad \min_{m_r, u_{ri}, y_h} \sum_{r\in\mathcal{R}} \sum_{i\in\mathcal{I}_r} \alpha^{\text{bun}} L_{ri} \overline{Q}_{ri}(u_{ri}) + \sum_{r\in\mathcal{R}} c_r^{\text{ves}} m_r + \sum_{h\in\mathcal{H}} c_h y_h \tag{39}$$

subject to constraints (18), (19), (21), (22), (24), and (25).

Algorithm 1 and the convexity of function $Q_{ri}(u_{ri})$ implies that

$$Q_{ri}(u_{ri}) - \bar{\varepsilon} \leqslant \overline{Q}_{ri}(u_{ri}) \leqslant Q_{ri}(u_{ri}), \quad \forall\, r \in \mathcal{R}, \quad \forall\, i \in \mathcal{I}_r, \quad \forall\, u_{ri} \in [U_{ri}^{\min}, U_{ri}^{\max}] \tag{40}$$

Therefore, by using the piecewise-linear function $\overline{Q}_{ri}(u_{ri})$ as a surrogate for $Q_{ri}(u_{ri})$, the total objective value error of [P3] with respect to the original model [P1] can be controlled within the tolerance level $\varepsilon$.

The convexity of function $Q_{ri}(u_{ri})$ further implies the convexity of $\overline{Q}_{ri}(u_{ri})$. Therefore [P3] can be transformed into an equivalent mixed-integer linear programming model [P4] by introducing new decision variables $Q_{ri}$:

$$[\text{P4}] \quad \min_{m_r, u_{ri}, y_h, Q_{ri}} \sum_{r\in\mathcal{R}} \sum_{i\in\mathcal{I}_r} \alpha^{\text{bun}} L_{ri} Q_{ri} + \sum_{r\in\mathcal{R}} c_r^{\text{ves}} m_r + \sum_{h\in H} c_h y_h \tag{41}$$

subject to constraints (18), (19), (21), (22), (24), and (25) and

$$Q_{ri} \geqslant \text{slope}_{rik} \times u_{ri} + \text{Q-intercept}_{rik}, \quad \forall\, r \in \mathcal{R}, \quad \forall\, i \in \mathcal{I}_r, \quad \forall\, k = 1, 2 \ldots K_{ri} \tag{42}$$

[P4] can be efficiently solved by state-of-art mixed-integer linear programming solvers such as CPLEX. Let the optimal objective value to the original mixed-integer nonlinear programming model [P1] be *Opt*. The optimal objective value to the approximation model [P4], denoted by *LB*, is a lower bound for *Opt*. Let the optimal solution to [P4] be $m_r^*$, $u_{ri}^*$, $y_h^*$, $Q_{ri}^*$. It is evident that $m_r = m_r^*$, $v_{ri} = 1/u_{ri}^*$, $y_h = y_h^*$ is a feasible solution to [P1], hence an upper bound for *Opt* can be determined by

$$UB = \sum_{r\in\mathcal{R}} \sum_{i\in I_r} \alpha^{\text{bun}} L_{ri} g_{ri}(1/u_{ri}^*) + \sum_{r\in\mathcal{R}} c_r^{\text{ves}} m_r^* + \sum_{h\in\mathcal{H}} c_h y_h^* \tag{43}$$

According to the piecewise-linear approximation scheme, it follows that

$$LB \leqslant Opt \leqslant UB \leqslant LB + \varepsilon \tag{44}$$

## 5. A case study

### 5.1. Description of parameter settings

To evaluate the applicability of the proposed model and the efficiency of the algorithm, we use a real-case example provided by a global liner shipping company. This example has 46 ports in an Asia–Europe–Oceania shipping network as shown in Fig. 4. There are a total of 652 O–D port pairs with container shipment demand and the overall demand is 22,054 TEUs/week. There are 3 types of ship and 11 ship routes, as shown in Tables 3 and 4, respectively. The 11 ship routes have 87 legs altogether. A total of 814 container routes for the 652 O–D port pairs in the shipping network are provided by the global liner shipping company. The load cost, discharge cost, and transshipment cost is assumed to be the same for all the 46 ports at 60 USD/TEU, 60 USD/TEU, and 100 USD/TEU, respectively. The container handling efficiency is assumed to be the same for all ports and is only related to ship type, as shown in Table 3. The pilotage in and out of any port by any ship is 4 h. The coefficients $a$ and $b$ for daily bunker consumption function (1) on each voyage leg is calibrated using the data provided by the

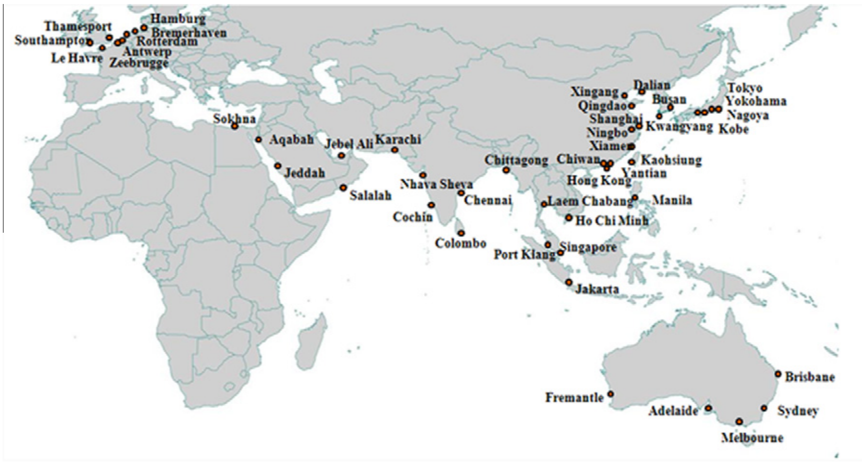


**Fig. 4.** Fourty-six ports in the case study. *Source*: Wang and Meng (2011).

**Table 3**
Ship fleet.

| Ship type (TEUs) | 3000 | 5000 | 10,000 |
|---|---|---|---|
| Min speed (knot) | 15 | 20 | 21 |
| Max speed (knot) | 23 | 26 | 30 |
| Container move per hour | 85 | 95 | 120 |
| Time for pilotage in and out of a port (hr) | 4 | 4 | 4 |
| Weekly operating cost (1000 USD) | 76.9 | 115.4 | 173.1 |

**Table 4**
Ship route.

| No. | Ship type | Ports of call |
|---|---|---|
| 1 | 5000-TEU | Singapore → Brisbane → Sydney → Melbourne → Adelaide → Fremantle |
| 2 | 5000-TEU | Xiamen → Chiwan → Hong Kong → Singapore → Port Klang → Salalah → Jeddah → Aqabah → Salalah → Singapore |
| 3 | 3000-TEU | Yokohama → Tokyo → Nagoya → Kobe → Shanghai |
| 4 | 3000-TEU | Ho Chi Minh → Laem Chabang → Singapore → Port Klang |
| 5 | 3000-TEU | Brisbane → Sydney → Melbourne → Adelaide → Fremantle → Jakarta → Singapore |
| 6 | 3000-TEU | Manila → Kaohsiung → Xiamen → Hong Kong → Yantian → Chiwan → Hong Kong |
| 7 | 3000-TEU | Dalian → Xingang → Qingdao → Shanghai → Ningbo → Shanghai → Kwangyang → Busan |
| 8 | 3000-TEU | Chittagong → Chennai → Colombo → Cochin → Nhava Sheva → Cochin → Colombo → Chennai |
| 9 | 5000-TEU | Sokhna → Aqabah → Jeddah → Salalah → Karachi → Jebel Ali → Salalah |
| 10 | 10000-TEU | Southampton → Thamesport → Hamburg → Bremerhaven → Rotterdam → Antwerp → Zeebrugge → Le Havre |
| 11 | 10000-TEU | Southampton → Sokhna → Salalah → Colombo → Singapore → Hong Kong → Xiamen → Shanghai → Busan → Dalian → Xingang → Qingdao → Shanghai → Hong Kong → Singapore → Colombo → Salalah |

global liner shipping company. The mixed-integer nonlinear programming model [P1] has a total of 11 integer decision variables $m_r$ and 87 + 814 = 901 continuous decision variables $v_{ri}$ and $y_h$. The total number of constraints is 11 + 87 + 652 + 2 × 87 = 924. The mixed-integer linear programming model [P4] has an additional 87 continuous decision variables $Q_{ri}$ and a number of approximation constraints (42). [P4] is solved by CPLEX-12.1 running on a 3 GHz Dual Core PC with 4 GB of RAM.

We set the absolute objective value tolerance $\varepsilon$ at 0.01 ($10^6$ USD/week) and solve the model [P4] with different bunker price settings. Given the bunker price $\alpha^{bun}$, we first calculate $\bar{\varepsilon}$ according to Eq. (29). After that, we obtain the approximation constraints (42) using the proposed algorithm for each of the 87 voyage legs in the shipping network. With these constraints, we can formulate model [P4], which is subsequently solved by CPLEX. The objective value of [P4], *LB*, is a lower bound of the original problem, and an upper bound, *UB*, can also be obtained by Eq. (43).

### 5.2. Result analysis

Table 5 shows the computational results regarding the number of approximation constraints (42), the CPU time used to solve the mixed-integer linear programming model [P4], the *LB* ($10^6$ USD/week), *UB*, and their relative difference. We ob-

**Table 5**
Computational results.

| Bunker price (USD/ton) | Number of constraints (42) | CPU time (s) | *LB* | *UB* | $(UB-LB)/LB$ (%) |
|---|---|---|---|---|---|
| 300 | 398 | 0.125 | 10.491 | 10.497 | 0.06 |
| 400 | 453 | 0.047 | 11.157 | 11.162 | 0.05 |
| 500 | 497 | 0.047 | 11.822 | 11.828 | 0.05 |
| 600 | 546 | 0.047 | 12.488 | 12.493 | 0.04 |
| 700 | 585 | 0.062 | 13.136 | 13.140 | 0.03 |
| 800 | 620 | 0.063 | 13.772 | 13.776 | 0.03 |
| 900 | 655 | 0.047 | 14.398 | 14.401 | 0.02 |
| 1000 | 692 | 0.063 | 15.023 | 15.027 | 0.02 |

serve that the proposed algorithm generates a piecewise-linear approximation function with a moderate number of pieces. Considering that there are 87 voyage legs, less than 10 pieces are needed to approximate $Q_{ri}(u_{ri})$. As a consequence, [P4] can be efficiently solved (less than 0.2 s). By setting $\varepsilon$ at 0.01, we can see that $UB - LB$ is indeed not greater than 0.01, which is consistent with (44). The setting of $\varepsilon$ is actually very tight: the relative difference of *LB* and *UB* is less than 0.1% for all bunker prices.

Table 6 reports the bunker cost ($10^6$ USD/week), ship cost, and the number of each type of ship deployed with the bunker price varying from 300 to 1000 USD/ton. It is evident that when the bunker price is high, more ships are deployed at the optimal solution in order to lower down the sailing speed and control bunker consumption. Our model provides the optimal trade-off between bunker cost and ship cost.

**Table 6**
Ship number and ship cost at different bunker prices.

| Bunker price (USD/ton) | Cost ($10^6$ USD/week) | | Ship number | | | |
|---|---|---|---|---|---|---|
| | Bunker | Ship | 1500-TEU | 3000-TEU | 5000-TEU | Sum |
| 300 | 1.992 | 3.577 | 9 | 10 | 10 | 29 |
| 400 | 2.659 | 3.577 | 9 | 10 | 10 | 29 |
| 500 | 3.324 | 3.577 | 9 | 10 | 10 | 29 |
| 600 | 3.990 | 3.577 | 9 | 10 | 10 | 29 |
| 700 | 4.445 | 3.769 | 10 | 11 | 10 | 31 |
| 800 | 5.082 | 3.769 | 10 | 11 | 10 | 31 |
| 900 | 5.630 | 3.846 | 11 | 11 | 10 | 32 |
| 1000 | 6.256 | 3.846 | 11 | 11 | 10 | 32 |

**Table 7**
Optimal sailing speed on each leg of ship route 1 at the bunker price 800 USD/ton.

| Leg | 1 Singapore→ | 2 Brisbane→ | 3 Sydney→ | 4 Melbourne→ | 5 Adelaide→ | 6 Fremantle→ |
|---|---|---|---|---|---|---|
| $a$ ($\times 10^{-2}$) | 1.296 | 1.326 | 1.293 | 1.215 | 1.260 | 1.254 |
| $b$ | 2.958 | 2.970 | 2.436 | 2.928 | 2.442 | 2.538 |
| Speed (knot) | 20.0 | 20.0 | 26.0 | 20.0 | 26.0 | 23.3 |

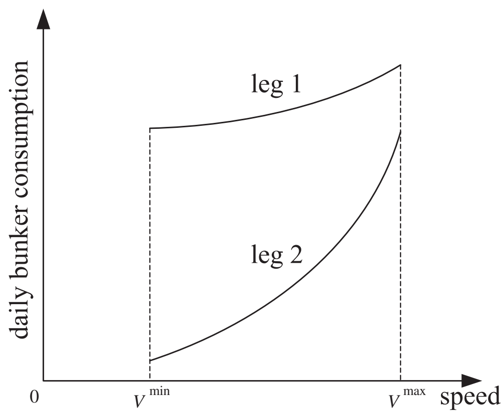


**Fig. 5.** A counter-example.

We further examine the optimal sailing speed structure. Table 7 shows the bunker consumption coefficients *a* and *b* and the optimal sailing speed on each leg of ship route 1 at the bunker price 800 USD/ton. We observe that at the same sailing speed, the daily bunker consumptions on legs 1 and 2 are higher than legs 3, 5, 6 since both coefficients *a* and *b* on legs 1 and 2 are larger than legs 3, 5, 6, and the optimal sailing speeds on legs 1 and 2 are lower than legs 3, 5, 6. However, one should note that higher daily bunker consumption does not necessarily mean lower sailing speed. Suppose that a ship route has two legs with bunker consumption function shown in Fig. 5. Evidently, leg 1 has higher bunker consumption than leg 2 at the same speed. However, the same speed increment would result in a much more dramatic increase in bunker consumption on leg 2 than leg 1. Hence, ships in general should sail at higher speed on leg 1 and lower speed on leg 2. In fact, the optimal sailing speed is mainly related to the sensitivity (derivative) of bunker consumption to speed, rather than the absolute bunker consumption value. In Table 7, since both coefficients *a* and *b* on legs 1 and 2 are larger than legs 3, 5, 6, the bunker consumption on legs 1 and 2 are more sensitive to speed than legs 3, 5, 6.

## 6. Conclusions

This paper calibrated the bunker consumption – sailing speed relation for container ships using historical operating data from a global liner shipping company. Results show that the extensively used third power relationship is indeed a good approximation. Therefore, the third power relation can be used if not enough historical data are available. Once enough historical data are available for the calibration purpose, a more accurate bunker consumption function should be used. The bunker consumption – sailing speed relation is also dependent on voyage legs. Therefore, this paper investigated the optimal sailing speed of container ships on each leg of each ship route in a liner shipping network while considering transshipment and container routing. It is formulated as a mixed-integer nonlinear programming model. In view of the convexity, non-negativity, and univariate properties of the bunker consumption – sailing speed function, an efficient outer-approximation method is proposed to obtain an $\varepsilon$-optimal solution with a predetermined optimality tolerance level $\varepsilon$. The proposed model and algorithm is applied to a real case study for a global liner shipping company.

The contributions of this paper to the literature are twofold. First, we calibrated the bunker consumption – sailing speed relation using historical operating data. Unlike many of the studies that use the third power relationship, we argue that once enough historical data are available for regression, a more accurate bunker consumption function should be adopted. Moreover, regression analysis shows that bunker consumption is also dependent on voyage legs, which contradicts the assumption of many studies.

Second, we propose the sailing speed optimization problem for container ships in a liner shipping network. This is a practical research issue arising in the liner shipping industry since (i) the bunker price is much higher than e.g. 10 years ago and (ii) green shipping has drawn much attention and low bunker consumption means less pollutant. To address this problem, a novel outer-approximation algorithm is proposed. The proposed algorithm is exact in that it obtains an $\varepsilon$-optimal solution and at the same time is very efficient. Moreover, the practical consideration of bunker consumption functions on different voyage legs is incorporated.

Finally, it should be mentioned that besides optimizing the sailing speed from the viewpoint of liner shipping companies, the proposed outer-approximation algorithm can also be used to examine the joint berth planning and sailing speed control problem (Golias et al., 2009, 2010; Du et al., 2011). Since the berth planning problem is already NP-hard, it is important to have efficient algorithms for addressing the nonlinearity of bunker consumption function.

## Acknowledgements

The authors would like to thank an anonymous reviewer for her/his valuable comments and suggestions. This study is supported by the research Grants – WBS No. R-264-000-244-720 and WBS No. R-302-000-014-720 – from the NOL Fellowship Programme of Singapore.

## References

Alvarez, J.F., Longva, T., Engebrethsen, E.S., 2010. A methodology to assess vessel berthing and speed optimization policies. Maritime Economics & Logistics 12, 327–346.

Christiansen, M., Fagerholt, K., Ronen, D., 2004. Ship routing and scheduling: status and perspectives. Transportation Science 38 (1), 1–18.

Corbett, J.J., Wang, H., Winebrake, J.J., 2010. The effectiveness and costs of speed reductions on emissions from international shipping. Transportation Research 14D, 593–598.

Du, Y., Chen, Q., Quan, X., Long, L., Fung, R.Y.K., 2011. Berth allocation considering fuel consumption and vessel emissions. Transportation Research 47E, 1021–1037.

Gelareh, S., Meng, Q., 2010. A novel modeling approach for the fleet deployment problem within a short-term planning horizon. Transportation Research 46E, 76–89.

Gelareh, S., Nickel, S., Pisinger, D., 2010. Liner shipping hub network design in a competitive environment. Transportation Research 46E, 991–1004.

Gelareh, S., Pisinger, D., 2011. Fleet deployment, network design and hub location of liner shipping companies. Transportation Research 47E, 947–964.

Golias, M.M., Saharidis, G.K., Boile, M., Theofanis, S., Ierapetritou, M.G., 2009. The berth allocation problem: optimizing vessel arrival time. Maritime Economics & Logistics 11, 358–377.

Golias, M.M., Boile, M., Theofanis, S., Efstathiou, C., 2010. The berth scheduling problem: maximizing berth productivity and minimizing fuel consumption and emissions production. Transportation Research Record 2166, 20–27.

Lang, N., Veenstra, A., 2010. A quantitative analysis of container vessel arrival planning strategies. OR Spectrum 32, 477–499.

Meng, Q., Wang, T., 2010. A chance constrained programming model for short-term liner ship fleet planning problems. Maritime Policy and Management 37 (4), 329–346.
Meng, Q., Wang, S., 2011a. Liner shipping service network design with empty container repositioning. Transportation Research 47E, 695–708.
Meng, Q., Wang, T., 2011b. A scenario-based dynamic programming model for multi-period liner ship fleet planning. Transportation Research 47E, 401–413.
Meng, Q., Wang, S., 2011c. Optimal operating strategy for a long-haul liner service route. European Journal of Operational Research 215, 105–114.
Notteboom, T.E., 2006. The time factor in liner shipping services. Maritime Economics and Logistics 8, 19–39.
Notteboom, T.E., Vernimmen, B., 2009. The effect of high fuel costs on liner service configuration in container shipping. Journal of Transport Geography 17, 325–337.
Ronen, D., 1982. The effect of oil price on the optimal speed of ships. Journal of the Operational Research Society 33, 1035–1040.
Ronen, D., 1993. Ship scheduling: the last decade. European Journal of Operational Research 71, 325–333.
Ronen, D., 2011. The effect of oil price on containership speed and fleet size. Journal of the Operational Research Society 62, 211–216.
Shintani, K., Imai, A., Nishimura, E., Papadimitriou, S., 2007. The container shipping network design problem with empty container repositioning. Transportation Research 43E, 39–59.
UNCTAD, Review of Maritime Transportation, 2010. Paper presented at the United Nations Conference on Trade and Development. New York and Geneva. <http://www.unctad.org/en/docs/rmt2010_en.pdf> (accessed 25.06.11).
Vernimmen, B., Dullaert, W., Engelen, S., 2007. Schedule unreliability in liner shipping: origins and consequences for the hinterland supply chain. Maritime Economics and Logistics 9, 193–213.
Wang, S., Meng, Q., 2011. Schedule design and container routing in liner shipping. Transportation Research Record 2222, 25–33.
Wang, S., Wang, T., Meng, Q., 2011. A note on liner ship fleet deployment. Flexible Services and Manufacturing Journal 23, 422–430.
Wang, S., Meng, Q., 2012. Liner ship fleet deployment with container transshipment operations. Transportation Research Part E 48, 470–484.